Original Article | Neuroimaging and Head & Neck

eISSN 2005-8330
https://doi.org/10.3348/kjr.2024.0177
Korean J Radiol 2024;25(10):913-923

Korean Journal of Radiology
KJR

Prospective Comparison of FOCUS MUSE and Single-Shot Echo-Planar Imaging for Diffusion-Weighted Imaging in Evaluating Thyroid-Associated Ophthalmopathy

YunMeng Wang[1,2]*, YuanYuan Cui[2]*, JianKun Dai[3], ShuangShuang Ni[2], TianRan Zhang[2], Xin Chen[2], QinLing Jiang[2], YuXin Cheng[2], YiChuan Ma[4], Tuo Li[5], Yi Xiao[2]

[1]Graduate School of Bengbu Medical University, Bengbu, China
[2]Department of Radiology, Second Affiliated Hospital of Naval Medical University, Shanghai, China
[3]GE Healthcare, Beijing, China
[4]Department of Radiology, The First Affiliated Hospital of Bengbu Medical University, Bengbu, China
[5]Department of Endocrinology, Changzheng Hospital, Shanghai, China

Objective: To prospectively compare single-shot (SS) echo-planar imaging (EPI) and field-of-view optimized and constrained undistorted single-shot multiplexed sensitivity-encoding (FOCUS MUSE) for diffusion-weighted imaging (DWI) in evaluating thyroid-associated ophthalmopathy (TAO).

Materials and Methods: SS EPI and FOCUS MUSE DWIs were obtained from 39 patients with TAO (18 male; mean ± standard deviation: 48.3 ± 13.3 years) and 26 healthy controls (9 male; mean ± standard deviation: 43.0 ± 18.5 years). Two radiologists scored the visual image quality using a 4-point Likert scale. The image quality score, signal-to-noise ratio (SNR), contrast-to-noise ratio (CNR), and apparent diffusion coefficient (ADC) of extraocular muscles (EOMs) were compared between the two DWIs. Differences in the ADC of EOMs were also evaluated. The performance of discriminating active from inactive TAO was assessed using receiver operating characteristic curves. The correlation between ADC and clinical activity score (CAS) was analyzed using Spearman correlation.

Results: Compared with SS EPI DWI, FOCUS MUSE DWI demonstrated significantly higher image quality scores ($P < 0.001$), a higher SNR and CNR on the lateral rectus muscle (LRM) and medial rectus muscle (MRM) ($P < 0.05$), and a non-significant difference in the ADC of the LRM and MRM. Active TAO showed higher ADC than inactive TAO and healthy controls with both SS EPI and FOCUS MUSE DWIs ($P < 0.001$). Inactive TAO and healthy controls did not show a significant ADC difference with both DWIs. Compared with SS EPI DWI, FOCUS MUSE DWI demonstrated better discrimination of active from inactive TAO (AUC: 0.925 vs. 0.779; $P = 0.007$). The ADC was significantly correlated with CAS in SS EPI DWI ($r = 0.391$, $P < 0.001$) and FOCUS MUSE DWI ($r = 0.645$, $P < 0.001$).

Conclusion: FOCUS MUSE DWI provides better images for evaluating EOMs and better performance in diagnosing active TAO than SS EPI DWI. The application of FOCUS MUSE will facilitate the DWI evaluation of TAO.

Keywords: Diffusion-weighted imaging; Thyroid-associated ophthalmopathy; Magnetic resonance imaging; Extraocular muscle

INTRODUCTION

Thyroid-associated ophthalmopathy (TAO) is an autoimmune inflammatory disease involving extraocular muscles (EOMs) and causing orbital fat expansion [1]. The active phase of TAO presents as EOM swelling, while the

Received: February 20, 2024 **Revised:** July 30, 2024 **Accepted:** August 2, 2024
*These authors contributed equally to this work.
Corresponding author: Yi Xiao, MD, PhD, Department of Radiology, Second Affiliated Hospital of Naval Medical University, No. 415 Fengyang Road, Huangpu District, Shanghai 200003, China
• E-mail: czyyxiaoyi@163.com

inactive phase presents as fibrosis [2]. Active TAO is treated with hormonal/anti-inflammatory drugs or radiotherapy, while inactive TAO is treated with surgical decompression [2]. Therefore, accurate staging of TAO is important to guide clinical treatment selection.

TAO activity is typically assessed using the clinical activity score (CAS), which is user-friendly; however, it depends on clinician experience and only inspects superficial anterior orbital structures [3]. The CAS does not evaluate deep posterior orbital structures, such as EOMs, which are significantly affected by TAO, and this could impact diagnostic accuracy. Mourits et al. [4] found that 36.0% of inactive TAO cases diagnosed with CAS responded to drug treatment, indicating a potential lack of sensitivity of the CAS. Therefore, using quantitative techniques to assess TAO-related structures may be beneficial for TAO staging.

Magnetic resonance imaging (MRI) aids in quantifying TAO, with diffusion-weighted imaging (DWI) analyzing water molecule diffusion [5-8]. Some studies [5,8-10] have used DWI to assess TAO-affected EOMs. The apparent diffusion coefficient (ADC) of EOMs was higher in patients with inflamed TAO than in healthy controls [5,8-10]. The commonly used DWI sequence employs single-shot (SS) echo-planar imaging (EPI) because it is fast and relatively insensitive to motion artifacts [11]. However, susceptibility distortions in the posterior orbits due to complex cave-bone-tissue organization can affect SS EPI DWI, impacting the visualization of EOMs, which in turn affects TAO evaluation. To mitigate the effects of magnetic field inhomogeneity, Ritchie et al. [7] used a half-Fourier SS fast spin-echo acquisition technique for DWI to reduce these susceptibility distortions. Fu et al. [12] reported that turbo gradient and spin echo BLADE DWI could improve EOM image quality for characterizing TAO activity. However, the partial-Fourier technique decreases signal-to-noise ratio (SNR) and limits field-of-view (FOV) and slice thickness because of the short-duration and high-amplitude gradient pulses [13], while BLADE DWI is time-consuming and imposes a high specific absorption rate [14]. Improved EPI-based imaging techniques may reduce susceptibility artifacts, maintain sufficient SNR, and provide high resolution with a relatively short scan time.

Reduced FOV DWI is an SS EPI-based technique that selectively excites a localized region using a two-dimensional tilted excitation, reducing imaging FOV and susceptibility artifacts [15,16]. It is commercially available as FOV optimized and constrained undistorted single-shot (FOCUS), ZOOMit, and ZOOM in GE, Siemens, and Philips systems. Previous studies have applied it to the spinal cord [17], prostate [18], breast [19], head and neck [20], and rectum [21]. Compared with SS EPI DWI, reduced FOV DWI reduces susceptibility artifacts, provides better anatomical detail, and improves lesion assessment [17-21].

Multiplexed sensitivity-encoding (MUSE) is another advanced EPI-based DWI technique that uses multiple excitations to correct field inhomogeneity-induced phase errors, resulting in a high SNR, high resolution, and reduced susceptibility artifacts [22]. Compared with SS EPI DWI, MUSE minimizes susceptibility artifacts and improves image quality for detecting lesions in the brain [22], bowel [23], liver [24], breast [25], and rectum [26]. Bai et al. [27] integrated the reduced FOV technique with MUSE and evaluated the performance of FOCUS MUSE for pancreas DWI. Thus, this prospective study aimed to compare FOCUS MUSE and SS EPI for DWI in evaluating TAO.

MATERIALS AND METHODS

Study Population

This prospective study was performed in line with the principles of the Declaration of Helsinki. Approval was granted by the Ethics Committee of our hospital (IRB No. 82170858). Before the MRI examination, all participants provided written informed consent by signing a consent form.

Inclusion criteria for patients with TAO were 1) age >18 years, and 2) no other orbital diseases and no history of orbital trauma. Exclusion criteria were 1) contraindications to MRI, 2) severe motion artifacts in the images, and 3) other orbital diseases, such as tumors in the orbit. Inclusion criteria for healthy controls were 1) age-matched individuals, 2) no history of orbital diseases, and 3) no abnormalities on orbital MRI. Finally, 39 patients clinically diagnosed with TAO (18 male; age: mean ± standard deviation: 48.3 ± 13.3 years) and 26 healthy controls (9 male; age: mean ± standard deviation: 43.0 ± 18.5 years) were between from April 2023 and August 2023. The study population flow chart is shown in Figure 1.

Clinical Assessment

Experienced endocrinologists scored each patient with TAO based on the CAS [2]. The scoring criteria included 1) spontaneous orbital pain, 2) eye pain when looking up/down, 3) eyelid congestion, 4) bulbar conjunctival congestion, 5) swelling of the lacrimal caruncle/fold,

https://doi.org/10.3348/kjr.2024.0177

Korean Journal of Radiology
KJR

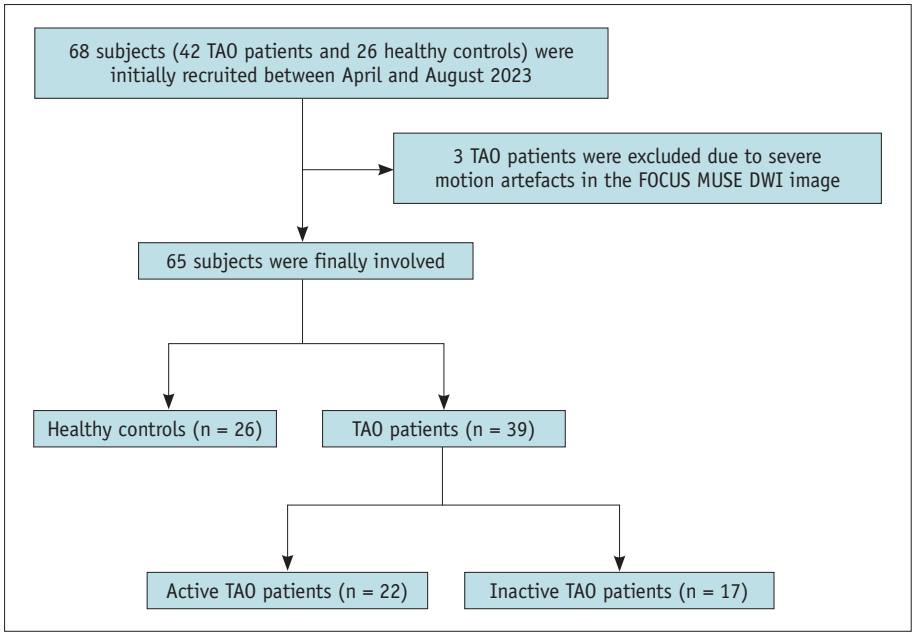

Fig. 1. Study population flow chart. TAO = thyroid-associated ophthalmopathy, FOCUS MUSE = field-of-view optimized and constrained undistorted single-shot multiplexed sensitivity-encoding, DWI = diffusion-weighted imaging

6) eyelid edema, and 7) bulbar conjunctival edema. Participants with a CAS of ≥3 and <3 were diagnosed as having active and inactive TAO, respectively [2].

MRI Acquisition

All MRI examinations were performed on a 3T MRI scanner (SIGNA Premier; GE Healthcare, Milwaukee, WI, USA) using a 21 channel head-and-neck combined coil. Participants, in supine position, were instructed to keep their eyes closed. The imaging region covered the entire orbit and optic chiasm using SS EPI and FOCUS MUSE DWIs, alongside T2-weighted imaging with short tau inversion recovery (T2WI-STIR) imaging for anatomical reference. The imaging parameters are shown in Table 1.

Visual Image Quality Assessment

Before imaging analysis, all DWI images were anonymized and presented in random order by one radiologist. Next, two other radiologists with 10 (reader 1) and 15 (reader 2) years of experience in head and neck radiology independently assessed the image quality. They were blinded to participant and image information. As shown in Table 2, susceptibility artifacts, sharpness of boundaries, geometric distortion, and overall image quality were visually assessed using a 4-point Likert scale (Supplementary Fig. 1) [27,28]. After a one-month washout, reader 1 re-assessed the visual image quality using the same method.

Table 1. Scanning parameters

	FOCUS MUSE DWI	SS EPI DWI	T2WI-STIR
TR, ms	4500	4500	4427
TE, ms	58.7	58.3	85
Field-of-view, cm	20.0 x 12.0	20.0 x 20.0	20.0 x 20.0
Matrix size	140 x 84	140 x 140	320 x 240
Slice thickness, mm	2.0	2.0	2.0
Number of slices	19	19	19
b-values, s/mm^2	0, 800	0, 800	-
NEX	2, 4	2, 4	2
Excitation mode	FOCUS	Selective	Selective
Number of shots	2	1	2
Total scan time	2 min 15 sec	1 min 8 sec	1 min 15 sec

FOCUS MUSE = field-of-view optimized and constrained undistorted single-shot multiplexed sensitivity-encoding, DWI = diffusion-weighted imaging, SS EPI = single-shot echo-planar imaging, T2WI-STIR = T2-weighted imaging with short tau inversion recovery, TR = repetition time, TE = echo time, NEX = number of excitations

Quantitative Image Quality Assessment and ADC Measurement

All quantitative objective image quality assessments were independently carried out by another two radiologists with three (reader 3) and eight (reader 4) years of experience in head and neck MRI. They were blinded to image and patient information. The SNR and contrast-to-noise ratio (CNR) of EOMs were used to evaluate DWI image quality. Regions of interest (ROIs) were manually defined on the DWI using

 https://doi.org/10.3348/kjr.2024.0177

Table 2. Visual image quality scoring criteria

Susceptibility artifacts
1. Heavy artifacts that severely affect structural display
2. Moderate artifacts, which affect the structural display to some extent
3. Mild artifacts that do not affect the structural display
4. No artifacts
Sharpness of boundaries
1. Anatomical structures are difficult to show
2. The anatomical structure has a clear outline and blurred edges
3. The anatomy shows well, the edges are less sharp
4. The anatomy is very clear, and the edges are sharp
Geometric distortion
1. Severe distortion and poor anatomical consistency with the geometry of the T2 sequence
2. Moderate distortion, good consistency with the geometric anatomical structure of T2 sequence
3. Mild distortion and high consistency with the geometric anatomy of the T2 sequence
4. No distortion
Overall image quality
1. Poor image quality and non-diagnostic
2. Image quality is average, diagnostic quality is slightly reduced
3. The image quality is good, and the diagnostic quality is barrier-free
4. Excellent image quality

the vendor-provided workstation (AW4.7; GE Healthcare), with T2WI-STIR used as a reference for delineation. ROIs of bilateral lateral rectus muscles (LRMs) and medial rectus muscles (MRMs) were drawn at the muscle belly's maximum cross-section, covering the central two-thirds of the area to mitigate the partial volume effect (Supplementary Fig. 2A-C). The ROIs were moved slightly to avoid artifacts at the belly of the EOMs. For EOMs that were severely distorted or incompletely visible, the adjacent slice was selected and the ROIs were delineated in the same manner (Supplementary Fig. 2D-G). Reader 3 re-evaluated all quantitative measurements after a one-month washout. The average and standard derivation (SD) of signal intensity (SI) within the EOM ROI were recorded as SI_{EOM} and SD_{EOM}, respectively. ROIs of the bilateral temporal muscle (TM) were manually drawn on the same section as EOMs to obtain the average (SI_{TM}) and standard deviation (SD_{TM}) of SI. The SNR and CNR were calculated using the following formula [29-31]:

$$SNR = SI_{EOM}/SD_{TM}$$

$$CNR = (SI_{EOM} - SI_{TM})/\sqrt{(SD_{EOM})^2 + (SD_{TM})^2}$$

An ADC map was calculated by fitting the DWI data using a mono-exponential function on the vendor-provided workstation (AW4.7; GE Healthcare). ADC was measured in both MRM and LRM, and the ROIs of EOMs defined above were copied to the ADC map. Reader 3 re-measured ADC values after a one-month washout. Then, the ADC values measured in MRMs from both eyes were used as representative measurements for each participant (i.e., two values per patient) for further analysis for the following reason. In clinical practice, according to the European Group on Graves' Orbitopathy, the left and right eyes are assessed separately [1,10,32]. The MRMs are more likely to be involved than the LRMs [33]. Therefore, this study used both of the participants' bilateral MRMs to distinguish TAO activity (i.e., the analysis was per muscle instead of per patient). All results other than intra- or inter-reader reliability were presented using data from the first pass by reader 3.

Statistical Analysis

Statistical analysis was performed using SPSS (version 25.0; IBM Corp., Armonk, NY, USA) and MedCalc (version 22.0; Mariakerke, Belgium). Normality was checked using the Kolmogorov-Smirnov test. Differences in age and sex between healthy controls and patients with TAO were compared using *t*-test and chi-square test. The inter- and intra-rater reliability for the image quality score, quantitative image quality parameters, and ADC were evaluated using kappa (κ) statistics, interclass correlation coefficient (ICC), and ICC, respectively. The κ and ICC values were interpreted as: <0.40, poor; 0.41–0.60, moderate; 0.61–0.80, good; and ≥0.81, excellent. The Wilcoxon signed rank test compared the image quality scores, SNR, CNR, and ADC between the FOCUS MUSE and SS EPI DWIs. The Kruskal-Wallis H test was used to compare the difference in EOM ADC among groups, and the Dunn-Bonferroni post hoc test was performed for significant pairwise comparisons. The correlation between the ADC and CAS of participants with TAO was analyzed using Spearman's coefficient. Receiver operating characteristic (ROC) curves evaluated the diagnostic performance of the ADC in differentiating active from inactive TAO, with the Delong test comparing two DWI sequences. $P < 0.05$ was considered statistically significant.

https://doi.org/10.3348/kjr.2024.0177

Korean Journal of Radiology
KJR

RESULTS

Sixty eight participants were initially recruited; however, three patients with TAO were excluded because of severe motion artifacts in FOCUS MUSE DWI. Therefore, 39 patients with TAO and 26 healthy controls were included for analysis. According to the CAS, 22 patients were diagnosed as having active TAO and 17 as having inactive TAO. No statistically significant difference in age (P = 0.204) and sex (P = 0.606) was observed between patients with TAO and healthy controls.

Both readers confirmed that the image quality of FOCUS MUSE DWI was better than that of SS EPI DWI (P < 0.001), presenting with fewer susceptibility artifacts and geometric distortion, better sharpness of boundaries, and an improved overall image quality (Table 3, Fig. 2). Both SS EPI and FOCUS MUSE DWIs demonstrated good to excellent inter-/intra-rater agreement (Table 3, κ > 0.7).

The SNR and CNR of EOMs for SS EPI and FOCUS MUSE DWIs presented with good to excellent intra-/inter-rater reliability, with ICC values ranging from 0.784 to 0.980 and from 0.846 to 0.959, respectively. The intra-/inter-rater reliability of the ADC value presented good to excellent reliability for SS EPI (ICC: 0.827–0.937) and FOCUS MUSE DWIs (ICC: 0.819–0.956) (Supplementary Table 1).

Table 3. Intra-rater and inter-rater agreement in visual image quality scoring in the extraocular muscles

	Visual score (n = 65)			κ value	
	Reader 1	Reader 1*	Reader 2	Intra-rater	Inter-rater
Susceptibility artifacts					
FOCUS MUSE DWI	3 (3–4)	3 (3–4)	3 (3–4)	0.948	0.813
SS EPI DWI	2 (2–3)	2 (2–3)	2 (2–3)	0.858	0.739
P	<0.001	<0.001	<0.001	-	-
Sharpness of boundaries					
FOCUS MUSE DWI	3 (3–4)	3 (3–4)	3 (3–4)	0.911	0.881
SS EPI DWI	2 (2–3)	2 (2–3)	2 (2–3)	0.764	0.763
P	<0.001	<0.001	<0.001	-	-
Geometric distortion					
FOCUS MUSE DWI	3 (3–4)	3 (3–4)	3 (3–4)	0.936	0.793
SS EPI DWI	2 (2–2)	2 (2–3)	2 (2–3)	0.883	0.713
P	<0.001	<0.001	<0.001	-	-
Overall image quality					
FOCUS MUSE DWI	4 (3–4)	4 (3–4)	4 (3–4)	0.974	0.871
SS EPI DWI	2 (2–3)	2 (2–3)	2 (2–3)	0.836	0.750
P	<0.001	<0.001	<0.001	-	-

Data are reported as median (interquartile range).
*Reader 1's second-time score.
FOCUS MUSE = field-of-view optimized and constrained undistorted single-shot multiplexed sensitivity-encoding, DWI = diffusion-weighted imaging, SS EPI = single-shot echo-planar imaging

The SNR (13.60 [10.83–16.52] vs. 8.91 [7.48–11.47]; P < 0.001) and CNR (2.20 [1.32–3.17] vs. 1.37 [0.52–2.13]; P < 0.001) of LRM were significantly higher in FOCUS MUSE DWI than in SS EPI DWI. Similarly, MRM presented significantly higher SNR (14.68 [12.01–18.27] vs. 12.20 [9.39–15.26]; P < 0.001) and CNR (2.95 [1.70–3.87] vs. 2.71 [1.83–3.64]; P = 0.031) in FOCUS MUSE DWI (Table 4). No significant difference in ADC was observed (Table 4, P > 0.05).

FOCUS MUSE DWI had a significantly higher representative ADC than SS EPI DWI in active TAO (P = 0.001); however, no significant difference in ADC was observed between the two techniques in healthy controls (P = 0.566) and inactive TAO (P = 0.427) (Table 5). SS EPI DWI showed that the ADC in patients with active TAO (1.59 [1.49–1.72]) was significantly higher than that in patients with inactive TAO (1.42 [1.34–1.50]; P < 0.001) and healthy controls (1.39 [1.27–1.50]; P < 0.001). Similarly, patients with active TAO (1.69 [1.60–1.77]) demonstrated significantly higher ADC than those with inactive TAO (1.39 [1.31–1.47]; P < 0.001) and healthy controls (1.42 [1.34–1.50]; P < 0.001) in FOCUS MUSE DWI (Table 5, Fig. 3). No significant ADC difference was observed between patients with inactive TAO and healthy controls (Fig. 3; P > 0.05).

Table 6 and Supplementary Figure 3 demonstrate that SS EPI and FOCUS MUSE DWIs could distinguish active from inactive TAO (P < 0.001). Compared with SS EPI DWI, FOCUS MUSE DWI demonstrated significantly better diagnostic performance (AUC: 0.925 vs. 0.779; P = 0.007) than SS EPI DWI. The ADC cut-off value for SS EPI DWI was 1.530 x 10^{-3}mm^2/s, with a sensitivity of 63.6% (28/44), a specificity of 88.2% (30/34), and an accuracy of 74.4% (58/78). The ADC cut-off value for FOCUS MUSE DWI was 1.476 x 10^{-3}mm^2/s, with a sensitivity of 100% (44/44), a specificity of 79.4% (27/34) and an accuracy of 91.0% (71/78).

The ADC of EOMs was significantly correlated with CAS for SS EPI DWI (r = 0.391, P < 0.001) and FOCUS MUSE DWI (r = 0.645, P < 0.001) (Fig. 4).

DISCUSSION

Our results revealed that the image quality of FOCUS MUSE DWI was superior to that of SS EPI DWI in terms of susceptibility artifacts, geometric distortions, sharpness

 https://doi.org/10.3348/kjr.2024.0177

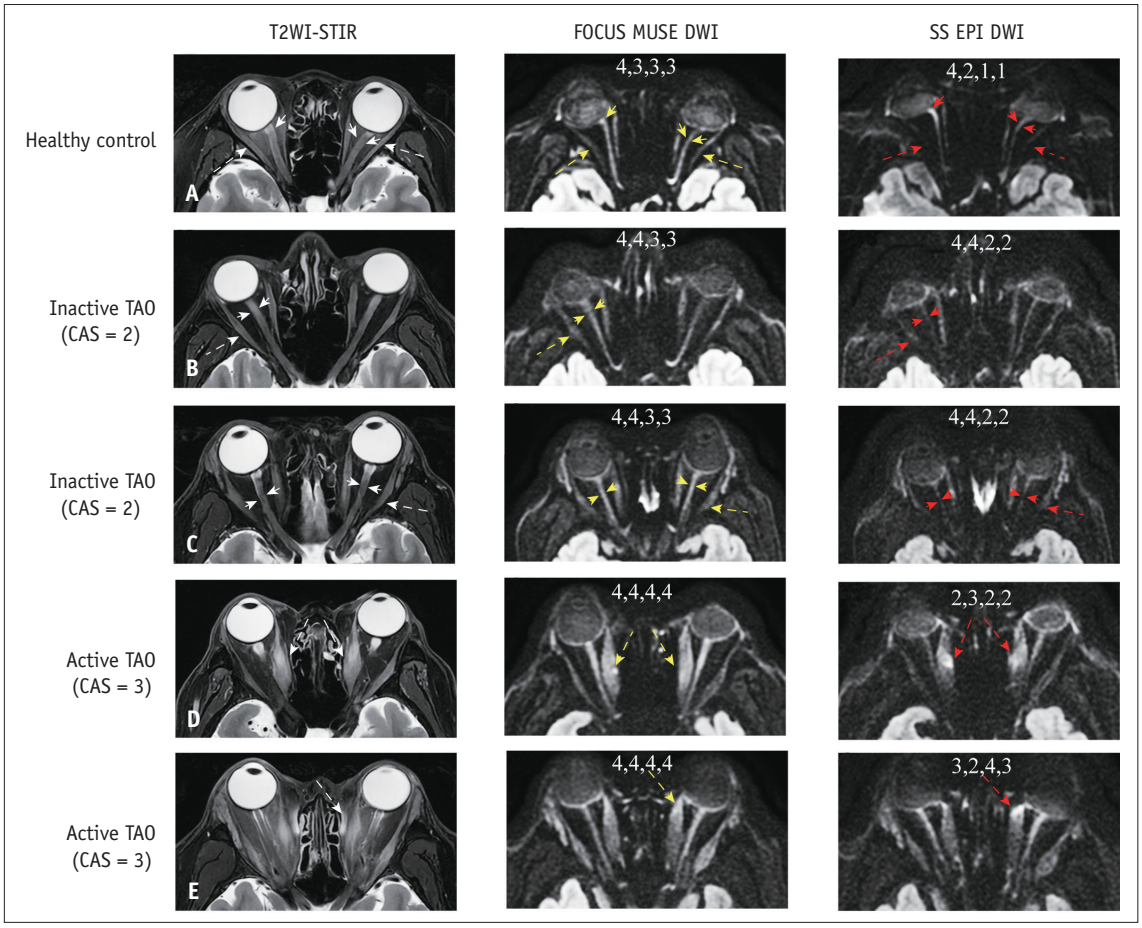

Fig. 2. Images from representative healthy controls and patients with inactive and active TAO. **A:** Middle image shows mild optic nerve distortion (yellow arrows) and clearly depicts LRMs (yellow dotted arrows). However, right image shows moderate optic nerve distortion (red arrows) and unclear LRMs (red dotted arrows). **B:** Middle image shows clear optic nerves (yellow arrows), and the LRM is delineated (yellow dotted arrow). Conversely, right image shows a blurry optic nerve (red arrows) and indistinct LRM (red dotted arrow). **C:** Middle image shows clear optic nerves (yellow arrows), and the LRM is displayed intact (yellow dotted arrow). In contrast, right image shows unclear optic nerves (red arrows) and an incomplete LRM (red dotted arrow). **D:** Middle image has no artifacts (yellow dotted arrows), whereas right image shows moderate artifacts in the MRMs (red dotted arrows). **E:** Middle image has no artifacts or distortions (yellow dotted arrow), while right image shows mild artifacts and distortion (red dotted arrow) in the MRM. The numbers within each diffusion-weighted image represent the visual image quality score of susceptibility artifacts, sharpness of boundaries, geometric distortion, and overall image quality. To clarify the structures marked by arrows in the DWI maps, T2WI-STIR images were referenced. Thus, the yellow and red arrows in FOCS MUSE DWI and SS EPI DWI match the structures indicated by white arrows in T2WI-STIR images, while the yellow and red dotted arrows correspond to the structures shown by white dotted arrows in T2WI-STIR images. TAO = thyroid-associated ophthalmopathy, LRM = lateral rectus muscle, MRM = medial rectus muscle, T2WI-STIR = T2-weighted imaging with short tau inversion recovery, FOCUS MUSE = field-of-view optimized and constrained undistorted single-shot multiplexed sensitivity-encoding, DWI = diffusion-weighted imaging, SS EPI = single-shot echo-planar imaging, CAS = clinical activity score

of boundaries, SNR, and CNR. FOCUS MUSE DWI exhibited superior diagnostic performance compared to SS EPI DWI regarding the distinction between active and inactive TAO, and a stronger correlation between ADC and CAS.

DWI can detect water proton motion, with ADC increasing in inflammatory tissues and decreasing in tissues with fat and fiber accumulation [5,9]. Active TAO is marked by inflammatory cell infiltration of orbital tissues, while inactive TAO presents with interstitial fibrosis and collagen deposition [2]. ADC is higher in patients with active TAO than in those with inactive TAO [8,9,32,34], which is consistent with our results. Nevertheless, patients with active TAO do not consistently exhibit significantly higher ADC than patients with inactive TAO [5,12,35]. This discrepancy is attributed to various factors, including the b-value used [5,12,35]. Yu et al. [10] and Liu et al. [9] reported that the ADC is significantly higher in patients with active TAO than in healthy controls. This is consistent

https://doi.org/10.3348/kjr.2024.0177

Korean Journal of Radiology
KJR

Table 4. Comparisons of SNR, CNR, and ADC between FOCUS MUSE and SS EPI DWI

	FOCUS MUSE DWI	SS EPI DWI	*P*
LRM (n = 130 muscles)			
SNR	13.60 (10.83–16.52)	8.91 (7.48–11.47)	<0.001
CNR	2.20 (1.32–3.17)	1.37 (0.52–2.13)	<0.001
ADC, x10^{-3}mm^2/s	1.51 (1.39–1.61)	1.48 (1.40–1.63)	0.674
MRM (n = 130 muscles)			
SNR	14.68 (12.01–18.27)	12.20 (9.39–15.26)	<0.001
CNR	2.95 (1.70–3.87)	2.71 (1.83–3.64)	0.031
ADC, x10^{-3}mm^2/s	1.44 (1.34–1.53)	1.42 (1.32–1.54)	0.166

Data are reported as median (interquartile range).
SNR = signal-to-noise ratio, CNR = contrast-to-noise ratio, ADC = apparent diffusion coefficient, FOCUS MUSE = field-of-view optimized and constrained undistorted single-shot multiplexed sensitivity-encoding, SS EPI = single-shot echo-planar imaging, DWI = diffusion-weighted imaging, LRM = lateral rectus muscle, MRM = medial rectus muscle

Table 5. Comparison of ADC (x10^{-3}mm^2/s) in MRMs between the two DWI techniques in healthy controls, active, and inactive TAO patients

	Healthy controls (n = 52)	Active TAO (n = 44)	Inactive TAO (n = 34)	*P*
FOCUS MUSE DWI	1.40 (1.31–1.46)	1.69 (1.60–1.77)	1.39 (1.31–1.47)	<0.001
SS EPI DWI	1.39 (1.27–1.50)	1.59 (1.49–1.72)	1.42 (1.34–1.50)	<0.001
P	0.566	0.001	0.427	

Data are reported as median (interquartile range).
ADC = apparent diffusion coefficient, MRM = medial rectus muscle, DWI = diffusion-weighted imaging, TAO = thyroid-associated ophthalmopathy, FOCUS MUSE = field-of-view optimized and constrained undistorted single-shot multiplexed sensitivity-encoding, SS EPI = single-shot echo-planar imaging

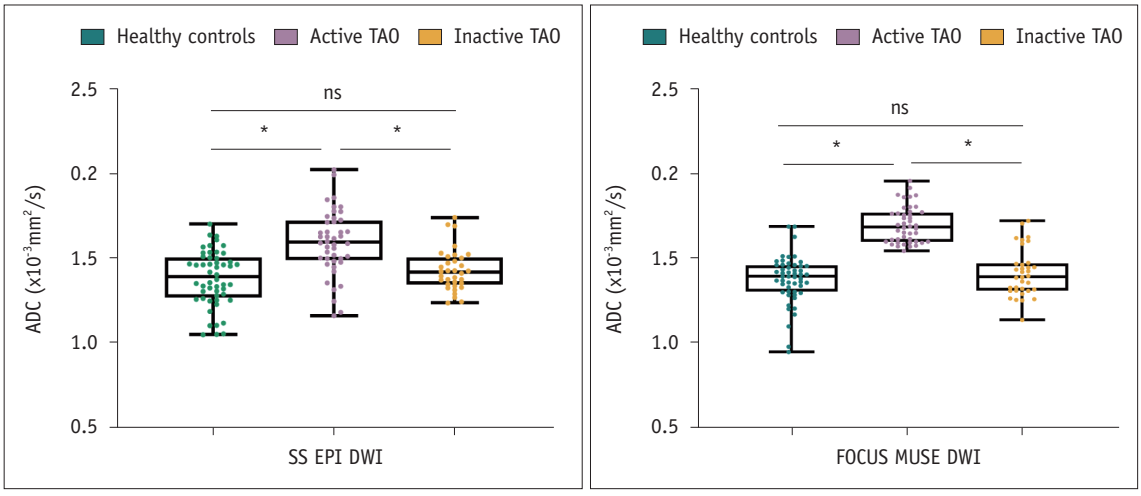

Fig. 3. Comparison of ADC values measured in the medial rectus muscles among healthy controls, patients with active TAO, and those with inactive TAO. *P < 0.001. ADC = apparent diffusion coefficient, TAO = thyroid-associated ophthalmopathy, SS EPI = single-shot echo-planar imaging, DWI = diffusion-weighted imaging, ns = no significant difference, FOCUS MUSE = field-of-view optimized and constrained undistorted single-shot multiplexed sensitivity-encoding

Table 6. Diagnostic performance of DWI for differentiating active from inactive TAO patients

	AUC	Cutoff, x10^{-3}mm^2/s	Sensitivity, %*	Specificity, %*	Accuracy, %*
FOCUS MUSE DWI	0.925	1.476	100 (44/44)	79.4 (27/34)	91.0 (71/78)
SS EPI DWI	0.779	1.530	63.6 (28/44)	88.2 (30/34)	74.4 (58/78)

TAO affects both eyes simultaneously or sequentially. Compared to the LRMs, the MRMs is more likely to be affected. Therefore, our study included the ADC values from bilateral MRMs to evaluate the diagnostic performance of DWIs in distinguishing the activity of TAO.
DWI = diffusion-weighted imaging, TAO = thyroid-associated ophthalmopathy, LRM = lateral rectus muscle, ADC = apparent diffusion coefficient, MRM = medial rectus muscle, AUC = area under curve, FOCUS MUSE = field-of-view optimized and constrained undistorted single-shot multiplexed sensitivity-encoding, SS EPI = single-shot echo-planar imaging

https://doi.org/10.3348/kjr.2024.0177

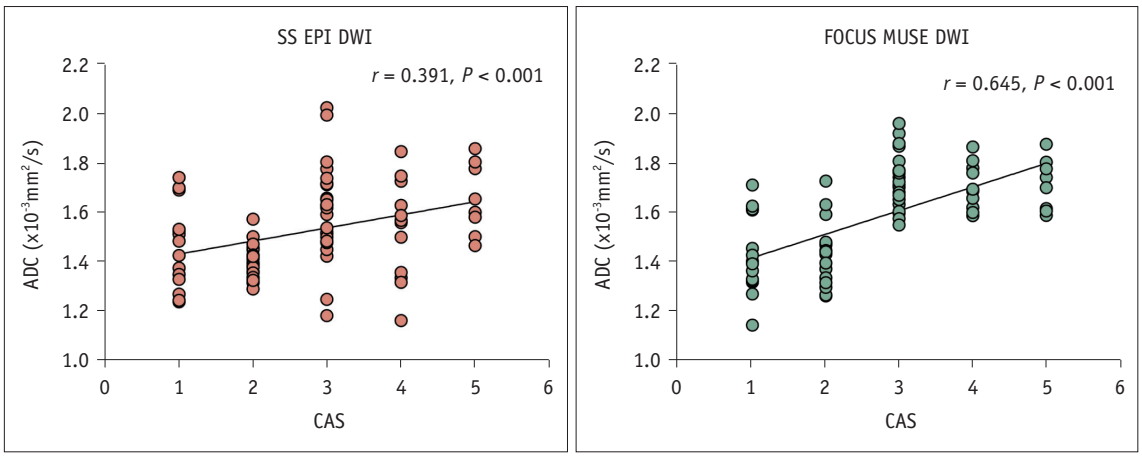

Fig. 4. Correlation between the ADC value measured in medial rectus muscles and CAS. ADC = apparent diffusion coefficient, CAS = clinical activity score, SS EPI = single-shot echo-planar imaging, DWI = diffusion-weighted imaging, FOCUS MUSE = field-of-view optimized and constrained undistorted single-shot multiplexed sensitivity-encoding

with the results in our study. Kilicarslan et al. [8] and Liu et al. [9] demonstrated that patients with inactive TAO have significantly higher ADC than healthy controls, which was not observed in our study. This may be because the b-value used in our study was 800 s/mm^2, while 1000 s/mm^2 was used in their studies. Our study and previous studies indicated that DWI is valuable for characterizing TAO; however, appropriate selection of b-value should be considered.

The CAS is the "gold standard" to grade TAO activity [36]. Quantitative evaluation using ADC correlates well with TAO activity [37]. Feeney et al. [34] and Politi et al. [5] demonstrated that the ADC of EOMs was significantly correlated with CAS. Similarly, our findings indicated a significant correlation between ADC and CAS, unlike the studies conducted by Kilicarslan et al. [8] and Liu et al. [9]. This could be attributed to the potential impact of subjective assessment and the b-value used [8,9]. Therefore, using DWI to quantitatively grade TAO activity appears feasible, and the optimal b-value should be considered, as mentioned above.

Several studies [5,8-10,32,34], including our study, have demonstrated the usefulness of DWI in characterizing TAO. However, SS EPI DWI presents a challenge for orbital imaging due to the intricate organization of cave-bone-tissue, leading to susceptibility distortion artifacts and signal loss [7,12,35]. Our study assessed the feasibility of FOCUS MUSE, an improved EPI-based DWI technique, to address limitations and found that FOCUS MUSE DWI outperformed SS EPI DWI in reducing distortion and improving SNR and CNR. This can be attributed to its integration of the advantages of reduced FOV and multi-shot techniques [27]. The increased image quality resulted in clearer depiction of EOMs. In addition, Besson et al. [11] showed that the correction of susceptibility distortions can increase the accuracy of ADC quantification. Iima et al. [38] illustrated that the low SNR of DWI can underestimate ADC and in turn affect the diagnostic performance. Therefore, the significant improvement in diagnostic performance with FOCUS MUSE DWI and its better correlation with CAS were likely attributable to reduced image distortion and enhanced SNR in our study.

Moreover, Hu et al. [32], using readout segmented EPI DWI, found that the moderate performance might be due to residual distortion and blur in EOMs, which could contribute to measurement variation. Turbo gradient and spin-echo BLADE acquisition is slower than EPI-based DWI and suffers from low SNR and image blurring [14]. To achieve sufficient image SNR, Fu et al. [12] selected a small b-value (600 s/mm^2), which may have had an impact on differentiating between active and inactive TAO. FOCUS MUSE is an EPI-based DWI, and it inherited the advantages of reduced FOV and multi-shot techniques. Our results illustrated a significant improvement in the differentiation of active and inactive EOMs in TAO and a strong correlation with CAS. This makes it a promising technique to obtain high resolution, high SNR, and less distorted DWI images for accurately characterizing TAO. Although FOCUS MUSE demonstrated significantly better performance than SS EPI, it doubled the scan time. This increase in scan time could potentially lead to an increase in motion artifacts, making the longer imaging time of FOCUS MUSE a limitation, compared to that of SS EPI. This limitation may be addressed by using advanced techniques,

https://doi.org/10.3348/kjr.2024.0177

Korean Journal of Radiology
KJR

such as deep learning reconstruction, to accelerate the acquisition without sacrificing SNR [39].

ADC quantitatively evaluates the diffusion process of water molecules and can reflect inflammation in tissues [5]. Our results showed that, with a b-value of 800 s/mm^2, the ADC cut-off values to discriminate active from inactive TAO were 1.476 x 10^{-3}mm^2/s and 1.530 x 10^{-3}mm^2/s for FOCUS MUSE and SS EPI DWIs, respectively. Abdel Razek et al. [40] reported that the ADC cut-off value was 1.690 x 10^{-3}mm^2/s using SS EPI DWI with a b-value of 500 s/mm^2. However, the ADC cut-off values were 1.444 x 10^{-3}mm^2/s and 1.780 x 10^{-3}mm^2/s in the studies by Kilicarslan et al. [8] and Liu et al. [9] with a higher b-value of 1000 s/mm^2. Our study and previous studies suggested that DWI was valuable in distinguishing active from inactive TAO. However, the ADC cut-off values varied among the studies mentioned above owing to the small sample size and different DWI acquisition techniques and b-values used. Further studies should be conducted to determine the optimal b-value for a specified DWI acquisition technique using a large sample size and to establish a reference ADC cut-off value for clinical practice.

This study had some limitations. First, the sample size in this prospective study was small. The effectiveness of FOCUS MUSE DWI requires further validation in larger clinical cohorts. Second, this study did not investigate whether FOCUS MUSE DWI was better than CAS in predicting treatment response. This is mainly due to the long follow-up time. We will conduct this study once follow-up data collection is completed. Third, the axial view was selected to acquire DWI images, which is inappropriate for visualizing the superior and inferior rectus muscles, thereby challenging ROI definition. In future studies, the coronal view will be used to assess the performance of the ADC of all EOMs in discriminating inactive from active TAO.

In conclusion, compared with SS EPI DWI, FOCUS MUSE significantly improved the image quality of orbital DWI, demonstrated significantly better performance in diagnosing active TAO, and was better correlated with CAS. Our study suggests that the application of FOCUS MUSE DWI would be beneficial for evaluating patients with TAO.

Supplement

The Supplement is available with this article at https://doi.org/10.3348/kjr.2024.0177.

Availability of Data and Material

The datasets generated or analyzed during the study are available from the corresponding author on reasonable request.

Conflicts of Interest

The authors have no potential conflicts of interest to disclose.

Author Contributions

Conceptualization: Yi Xiao. Data curation: YunMeng Wang, YuanYuan Cui, Xin Chen, QinLing Jiang, YuXin Cheng. Formal analysis: YunMeng Wang, YuanYuan Cui. Funding acquisition: Yi Xiao, Tuo Li. Investigation: YunMeng Wang, YuanYuan Cui, ShuangShuang Ni, TianRan Zhang. Methodology: YunMeng Wang, YuanYuan Cui. Supervision: JianKun Dai, YiChuan Ma. Writing—original draft: YunMeng Wang, YuanYuan Cui.

ORCID IDs

YunMeng Wang
https://orcid.org/0009-0008-2866-5377
YuanYuan Cui
https://orcid.org/0000-0003-3782-1315
JianKun Dai
https://orcid.org/0000-0002-2461-6737
ShuangShuang Ni
https://orcid.org/0009-0007-8083-3799
TianRan Zhang
https://orcid.org/0009-0001-9388-8779
Xin Chen
https://orcid.org/0009-0002-8173-8068
QinLing Jiang
https://orcid.org/0009-0007-2930-6598
YuXin Cheng
https://orcid.org/0009-0001-8969-9203
YiChuan Ma
https://orcid.org/0000-0003-4661-0034
Tuo Li
https://orcid.org/0000-0002-6691-7423
Yi Xiao
https://orcid.org/0000-0001-6758-3763

Funding Statement

This study has received funding from the National Key Research and Development Program of China (No. 2022YFC2410000 & No. 2022YFC2410002); the National

Natural Science Foundation of China (No. 82271994); the Military Commission health care special project (No. 22BJZ07); the National Health Commission capacity building and continuing Education center (No. YXFSC2022JJSJ010); the Shanghai Hospital Development Center (No. SHDC22022310-B); National Natural Science and Foundation of China (No. 82170858); Bengbu Medical University Postgraduate Research and Innovation Programme Project (No. Byycx23036).

Acknowledgments

First of all, I would like to give my heartfelt thanks to all the people who have ever helped me in this paper. My sincere and hearty thanks and appreciations go firstly to my supervisor, Mrs. Xiao Yi, whose suggestions and encouragement have given me much insight into these translation studies. It has been a great privilege and joy to study under her guidance and supervision. My gratitude to her knows no bounds. I am also extremely grateful to all my teachers and classmates who have kindly provided me assistance and companionship in the course of preparing this paper. Finally, I am really grateful to all those who devote much time to reading this thesis and give me much advice, which will benefit me in my later study.

REFERENCES

1. Burch HB, Perros P, Bednarczuk T, Cooper DS, Dolman PJ, Leung AM, et al. Management of thyroid eye disease: a consensus statement by the American Thyroid Association and the European Thyroid Association. *Thyroid* 2022;32:1439-1470
2. Barrio-Barrio J, Sabater AL, Bonet-Farriol E, Velázquez-Villoria Á, Galofré JC. Graves' ophthalmopathy: VISA versus EUGOGO classification, assessment, and management. *J Ophthalmol* 2015;2015:249125
3. Mourits MP, Koornneef L, Wiersinga WM, Prummel MF, Berghout A, van der Gaag R. Clinical criteria for the assessment of disease activity in Graves' ophthalmopathy: a novel approach. *Br J Ophthalmol* 1989;73:639-644
4. Mourits MP, Prummel MF, Wiersinga WM, Koornneef L. Clinical activity score as a guide in the management of patients with Graves' ophthalmopathy. *Clin Endocrinol (Oxf)* 1997;47:9-14
5. Politi LS, Godi C, Cammarata G, Ambrosi A, Iadanza A, Lanzi R, et al. Magnetic resonance imaging with diffusion-weighted imaging in the evaluation of thyroid-associated orbitopathy: getting below the tip of the iceberg. *Eur Radiol* 2014;24:1118-1126
6. Higashiyama T, Nishida Y, Morino K, Ugi S, Nishio Y, Maegawa H, et al. Use of MRI signal intensity of extraocular muscles to evaluate methylprednisolone pulse therapy in thyroid-associated ophthalmopathy. *Jpn J Ophthalmol* 2015;59:124-130
7. Ritchie AE, Lee V, Feeney C, Lingam RK. Using nonechoplanar diffusion-weighted MRI to assess treatment response in active Graves orbitopathy: a novel approach with 2 case reports. *Ophthalmic Plast Reconstr Surg* 2016;32:e67-e70
8. Kilicarslan R, Alkan A, Ilhan MM, Yetis H, Aralasmak A, Tasan E. Graves' ophthalmopathy: the role of diffusion-weighted imaging in detecting involvement of extraocular muscles in early period of disease. *Br J Radiol* 2015;88:20140677
9. Liu X, Su Y, Jiang M, Fang S, Huang Y, Li Y, et al. Application of magnetic resonance imaging in the evaluation of disease activity in Graves' ophthalmopathy. *Endocr Pract* 2021;27:198-205
10. Yu W, Zheng L, Shuo Z, Xingtong L, Mengda J, Lin Z, et al. Evaluation of extraocular muscles in patients with thyroid associated ophthalmopathy using apparent diffusion coefficient measured by magnetic resonance imaging before and after radiation therapy. *Acta Radiol* 2022;63:1180-1186
11. Besson FL, Fernandez B, Faure S, Mercier O, Seferian A, Blanchet É, et al. Diffusion-weighted imaging voxelwise-matched analyses of lung cancer at 3.0-T PET/MRI: reverse phase encoding approach for echo-planar imaging distortion correction. *Radiology* 2020;295:692-700
12. Fu Q, Liu D, Ma H, Zhou K, Yin T, Zheng C, et al. Turbo gradient and spin-echo BLADE-DWI for extraocular muscles in thyroid-associated ophthalmopathy. *J Clin Med* 2023;12:344
13. Semelka RC, Kelekis NL, Thomasson D, Brown MA, Laub GA. HASTE MR imaging: description of technique and preliminary results in the abdomen. *J Magn Reson Imaging* 1996;6:698-699
14. Li Z, Pipe JG, Lee CY, Debbins JP, Karis JP, Huo D. X-PROP: a fast and robust diffusion-weighted propeller technique. *Magn Reson Med* 2011;66:341-347
15. Tanabe M, Higashi M, Benkert T, Imai H, Miyoshi K, Kameda F, et al. Reduced field-of-view diffusion-weighted magnetic resonance imaging of the pancreas with tilted excitation plane: a preliminary study. *J Magn Reson Imaging* 2021;54:715-720
16. Riffel P, Michaely HJ, Morelli JN, Pfeuffer J, Attenberger UI, Schoenberg SO, et al. Zoomed EPI-DWI of the pancreas using two-dimensional spatially-selective radiofrequency excitation pulses. *PLoS One* 2014;9:e89468
17. Saritas EU, Cunningham CH, Lee JH, Han ET, Nishimura DG. DWI of the spinal cord with reduced FOV single-shot EPI. *Magn Reson Med* 2008;60:468-473
18. Korn N, Kurhanewicz J, Banerjee S, Starobinets O, Saritas E, Noworolski S. Reduced-FOV excitation decreases susceptibility artifact in diffusion-weighted MRI with endorectal coil for prostate cancer detection. *Magn Reson Imaging* 2015;33:56-62
19. Dong H, Li Y, Li H, Wang B, Hu B. Study of the reduced field-of-view diffusion-weighted imaging of the breast. *Clin Breast Cancer* 2014;14:265-271
20. Riffel P, Michaely HJ, Morelli JN, Pfeuffer J, Attenberger UI, Schoenberg SO, et al. Zoomed EPI-DWI of the head and neck with two-dimensional, spatially-selective radiofrequency

https://doi.org/10.3348/kjr.2024.0177

excitation pulses. *Eur Radiol* 2014;24:2507-2512
21. Peng Y, Tang H, Hu X, Shen Y, Kamel I, Li Z, et al. Rectal cancer invasiveness: whole-lesion diffusion-weighted imaging (DWI) histogram analysis by comparison of reduced field-of-view and conventional DWI techniques. *Sci Rep* 2019;9:18760
22. Chen NK, Guidon A, Chang HC, Song AW. A robust multi-shot scan strategy for high-resolution diffusion weighted MRI enabled by multiplexed sensitivity-encoding (MUSE). *Neuroimage* 2013;72:41-47
23. Chang HC, Chen G, Chung HW, Wu PY, Liang L, Juan CJ, et al. Multi-shot diffusion-weighted MRI with multiplexed sensitivity encoding (MUSE) in the assessment of active inflammation in Crohn's disease. *J Magn Reson Imaging* 2022;55:126-137
24. Kim YY, Kim MJ, Gho SM, Seo N. Comparison of multiplexed sensitivity encoding and single-shot echo-planar imaging for diffusion-weighted imaging of the liver. *Eur J Radiol* 2020;132:109292
25. Baxter GC, Patterson AJ, Woitek R, Allajbeu I, Graves MJ, Gilbert F. Improving the image quality of DWI in breast cancer: comparison of multi-shot DWI using multiplexed sensitivity encoding to conventional single-shot echo-planar imaging DWI. *Br J Radiol* 2021;94:20200427
26. El Homsi M, Bates DDB, Mazaheri Y, Sosa R, Gangai N, Petkovska I. Multiplexed sensitivity-encoding diffusion-weighted imaging (MUSE) in diffusion-weighted imaging for rectal MRI: a quantitative and qualitative analysis at multiple b-values. *Abdom Radiol (NY)* 2023;48:448-457
27. Bai Y, Pei Y, Liu WV, Liu W, Xie S, Wang X, et al. MRI: evaluating the application of FOCUS-MUSE diffusion-weighted imaging in the pancreas in comparison with FOCUS, MUSE, and single-shot DWIs. *J Magn Reson Imaging* 2023;57:1156-1171
28. Fu Q, Kong XC, Liu DX, Zhou K, Guo YH, Lei ZQ, et al. Turbo gradient and spin echo PROPELLER-diffusion weighted imaging for orbital tumors: a comparative study with readout-segmented echo-planar imaging. *Front Neurosci* 2021;15:755327
29. Mayer E, Herdman G, Burnett C, Kabala J, Goddard P, Potts MJ. Serial STIR magnetic resonance imaging correlates with clinical score of activity in thyroid disease. *Eye (Lond)* 2001;15(Pt 3): 313-318
30. Mayer EJ, Fox DL, Herdman G, Hsuan J, Kabala J, Goddard P, et al. Signal intensity, clinical activity and cross-sectional areas on MRI scans in thyroid eye disease. *Eur J Radiol* 2005;56:20-24
31. Tortora F, Prudente M, Cirillo M, Elefante A, Belfiore MP, Romano F, et al. Diagnostic accuracy of short-time inversion recovery sequence in Graves' ophthalmopathy before and after prednisone treatment. *Neuroradiology* 2014;56:353-361
32. Hu H, Chen L, Zhou J, Chen W, Chen HH, Zhang JL, et al. Multiparametric magnetic resonance imaging for differentiating active from inactive thyroid-associated ophthalmopathy: added value from magnetization transfer imaging. *Eur J Radiol* 2022;151:110295
33. Patrinely JR, Osborn AG, Anderson RL, Whiting AS. Computed tomographic features of nonthyroid extraocular muscle enlargement. *Ophthalmology* 1989;96:1038-1047
34. Feeney C, Lingam RK, Lee V, Rahman F, Nagendran S. Non-EPI-DWI for detection, disease monitoring, and clinical decision-making in thyroid eye disease. *AJNR Am J Neuroradiol* 2020;41:1466-1472
35. Hiwatashi A, Togao O, Yamashita K, Kikuchi K, Momosaka D, Honda H. Diffusion-weighted magnetic resonance imaging of extraocular muscles in patients with Grave's ophthalmopathy using turbo field echo with diffusion-sensitized driven-equilibrium preparation. *Diagn Interv Imaging* 2018;99:457-463
36. Bartalena L, Baldeschi L, Dickinson A, Eckstein A, Kendall-Taylor P, Marcocci C, et al. Consensus statement of the European Group on Graves' orbitopathy (EUGOGO) on management of GO. *Eur J Endocrinol* 2008;158:273-285
37. Lingam RK, Mundada P, Lee V. Novel use of non-echo-planar diffusion weighted MRI in monitoring disease activity and treatment response in active Grave's orbitopathy: an initial observational cohort study. *Orbit* 2018;37:325-330
38. Iima M, Partridge SC, Le Bihan D. Six DWI questions you always wanted to know but were afraid to ask: clinical relevance for breast diffusion MRI. *Eur Radiol* 2020;30:2561-2570
39. Lee KL, Kessler DA, Dezonie S, Chishaya W, Shepherd C, Carmo B, et al. Assessment of deep learning-based reconstruction on T2-weighted and diffusion-weighted prostate MRI image quality. *Eur J Radiol* 2023;166:111017
40. Abdel Razek AA, El-Hadidy M, Moawad ME, El-Metwaly N, El-Said AA. Performance of apparent diffusion coefficient of medial and lateral rectus muscles in Graves' orbitopathy. *Neuroradiol J* 2017;30:230-234

 https://doi.org/10.3348/kjr.2024.0177